JOC Article

Binding of Small Guest Molecules to Multivalent Receptors

Mattijs G. J. ten Cate, David N. Reinhoudt,* and Mercedes Crego-Calama*

Laboratory of Supramolecular Chemistry and Technology, MESA+ Institute for Nanotechnology, University of Twente, P.O. Box 217, 7500 AE Enschede, The Netherlands

m.cregocalama@utwente.nl

Received June 15, 2005

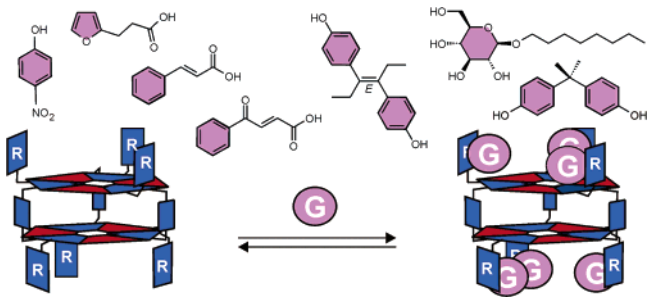

The complexation of phenol derivatives, aromatic carboxylic acids, and *n*-octylgalactopyranoside by hydrogen-bonded exo-receptors is described. The receptors are formed by self-assembly of differently functionalized calix[4]arene dimelamines with 5,5-diethyl barbiturate or butyl cyanurate. The multivalent complementary recognition site of the receptors is used very efficiently to complex multiple guests. A 1:6 binding mode was observed for phenol derivatives forming single hydrogen bonds with all six recognition sites of an ureido functionalized receptor assembly, while 1:3 complexation was observed for phenol derivatives which form two hydrogen bonds with two different ureido recognition sites of the same receptor. Aromatic carboxylic acids are complexed in a 1:6 ratio by receptors having six amino recognition sites. The complexation of *n*-octylgalactopyranoside by Gly-L-Ser functionalized receptors is also described, indicating that it is possible to use small peptidic fragments to complex biologically important molecules.

Introduction

Biochemical processes such as enzymatic action, molecular transport, genetic information and processing, and protein assembly all involve molecular recognition.[1] The exquisite recognition of an antigen by the antibody is just one example of the remarkable chemical control achieved by biological systems.[2] Compared to natural systems, most synthetic receptors[3] use only a limited number of weak interactions. In general, these receptors are able to bind single guest molecules such as cations,[4] anions,[5] or small neutral molecules.[6] However, there are essentially no examples of synthetic molecules that bind to a substrate with the strength or selectivity of an antibody.[2] To enhance binding strength and selectivity of natural receptors, multiple interactions have been used by combination of amino acids and nucleotides.[7] These multiple interactions (multivalency) display unique col-

* To whom correspondance should be addressed. Fax: +31 53 489 4645. Tel: +31 53 489 2978.

(1) (a) Page, M. I. *The Chemistry of Enzyme Action*; Elsevier: Amsterdam, The Netherlands, 1984. (b) Hulme, E. C. *Receptor Biochemistry: A Practical Approach*; Oxford University Press: New York, 1990. (c) Roberts, S. M. *Molecular Recognition: Chemical and Biochemical Problems*; Royal Society of Chemistry: Cambridge, England, 1989.

(2) Hamilton, A. D. *Nature*, **2002**, *418*, 375−376.

(3) (a) Conn, M. M.; Rebek, J., Jr. *Chem. Rev.* **1997**, *97*, 1647−1668. (b) Linton, B.; Hamilton, A. D. *Chem. Rev.* **1997**, *97*, 1669−1680. (c) Jacopozzi, P.; Dalcanale, E. *Angew. Chem., Int. Ed. Engl.* **1997**, *36*, 613−615. (d) Fujita, M. *Chem. Soc. Rev.* **1998**, *27*, 417−425. (e) Hartley, J. H.; James, T. D.; Ward, C. J. *Chem. Soc., Perkin Trans. 1* **2000**, 3155−3184. (f) Vysotsky, M. O.; Thondorf, I.; Böhmer, V. *Angew. Chem., Int. Ed.* **2000**, *39*, 1264−1267. (g) Rincon, A. M.; Prados, P.; De Mendoza, J. *J. Am. Chem.* **2001**, *123*, 3493−3498. (h) Umemoto, K.; Tsukui, H.; Kusukawa, T.; Biradha, K.; Fujita, M. *Angew. Chem., Int. Ed.* **2001**, *40*, 2620−2622. (i) Chen, J.; Körner, S.; Craig, S. L.; Rudkevich, D. M.; Rebek, J., Jr. *Nature* **2002**, *415*, 385−386. (j) Corbellini, F.; Fiammengo, R.; Timmerman, P.; Crego-Calama, M.; Versluis, K.; Heck, A. J. R.; Luyten, I.; Reinhoudt, D. N. *J. Am. Chem. Soc.* **2002**, *124*, 6569−6575.

(4) (a) Cram, D. J.; Kaneda, T.; Helgeson, R. C.; Brown, B.; Knobler, C. B.; Meverick, E.; Trueblood, K. N. *J. Am. Chem. Soc.* **1985**, *107*, 3645−3657. (b) Bell, T. W.; Khasanov, A. B.; Drew, M. G. B.; Filikov, A.; James, T. L. *Angew. Chem., Int. Ed.* **1999**, *38*, 2543−2547. (c) Chrisstoffels, L. A. J.; De Jong, F.; Reinhoudt, D. N.; Sivelli, S.; Gazzola, L.; Casnati, A.; Ungaro, R. *J. Am. Chem. Soc.* **1999**, *121*, 10142−10151. (d) Schalley, C. A.; Castellano, R. K.; Brody, M. S.; Rudkevich, D. M.; Siuzdak, G.; Rebek, J., Jr. *J. Am. Chem. Soc.* **1999**, *121*, 4568−4579. (e) Shivanyuk, A.; Paulus, E. F.; Böhmer, V. *Angew. Chem. Int. Ed.* **1999**, *38*, 2906−2909. (f) Cho, Y. L.; Rudkevich, D. M.; Rebek, J., Jr. *J. Am. Chem. Soc.* **2000**, *122*, 9868−9869.

10.1021/jo051218c CCC: $30.25
Published on Web 09/22/2005

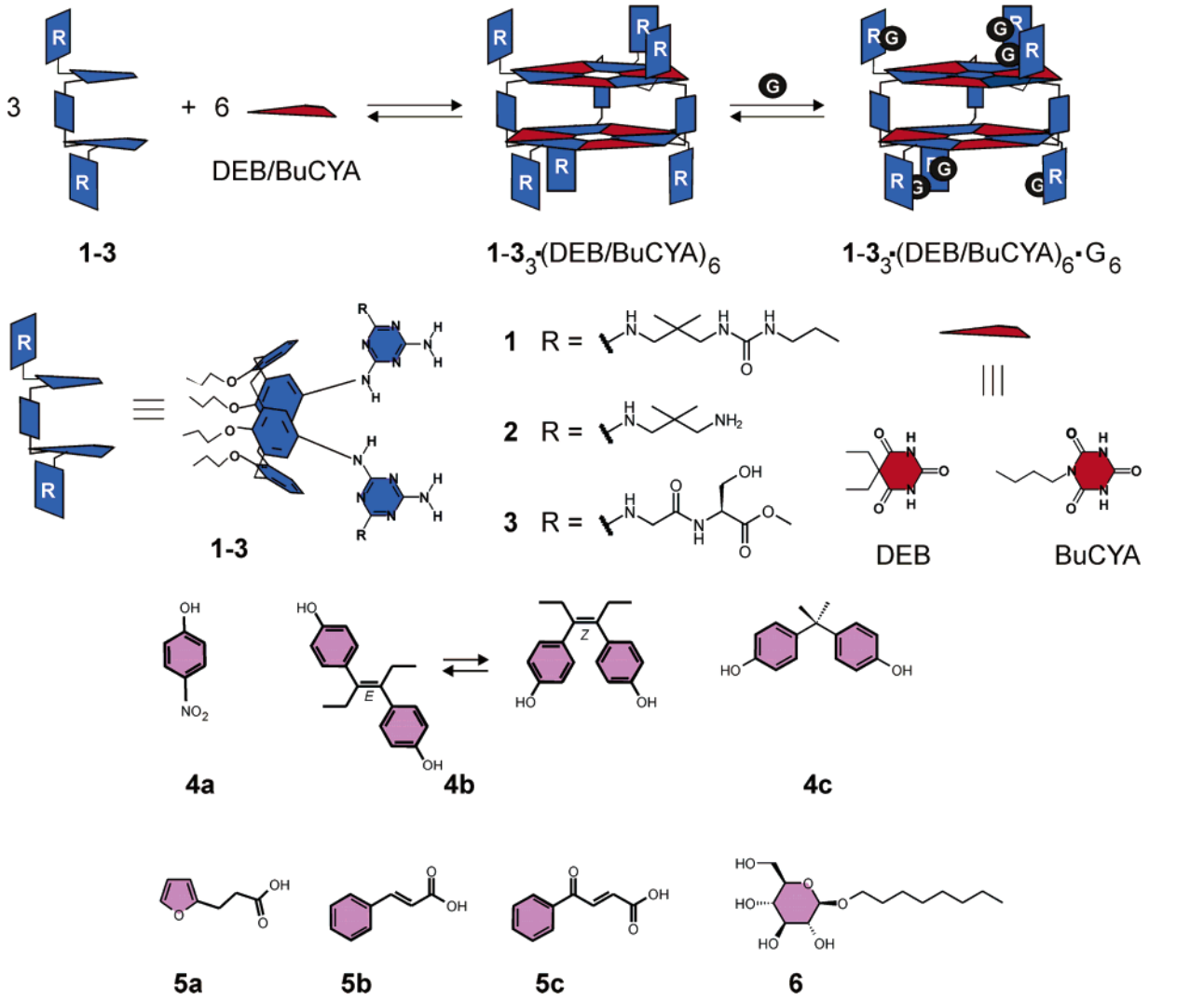

FIGURE 1. Schematic representation (side view) of exo-recognition of six guests (G) by double rosette assemblies (top), and molecular structures of dimelamines **1**−**3**, DEB and BuCYA, and guest molecules **4a**−**c**, **5a**−**c**, and **6** (bottom).

lective properties compared to the properties of their monovalent binding constituents.

Multivalent recognition of substrates with strong and selective binding requires a large contact area and a sufficient number of complementary recognition sites. This mode of molecular recognition is observed at the antibody−antigen interface.[8]

Here we describe the synthesis, conformation, and complexation behavior of hydrogen-bonded double rosettes with different recognition sites at the exterior part of the assemblies that are used as exo-receptors. These double rosettes are assembled from calix[4]arene dimelamines **1**−**3** with 2 equiv of 5,5-diethyl barbituric acid (DEB) or *n*-butyl cyanurate (BuCYA), via formation of 36 hydrogen bonds (Figure 1). The melamine units of these assemblies are functionalized with ureido (**1**), amino (**2**), or L-serine (**3**) moieties to recognize phenols, aromatic carboxylic acids, and carbohydrate derivatives, respectively. As a result, recognition sites are located at the periphery of the double rosettes (exo-recognition) (Figure 1).

In principle, these exo-receptors could complex two large guests[9] (i.e. one at the bottom and one at the top of the double rosettes), but here the focus is on binding multiple small guest molecules to these multivalent

(5) (a) Tobey, S. L.; Anslyn, E. V. *J. Am. Chem. Soc.* **2003**, 125, 10963−10970. (b) Gale, P. A. *Coord. Chem. Rev.* **2001**, *213*, 79−128. (c) Suksai, C.; Tuntulani, T. *Chem. Soc. Rev.* **2003**, *32*, 192−202. (d) Sessler, J. L.; Camiolo, S.; Gale, P. A. *Coord. Chem. Rev.* **2003**, *240*, 17−55. (e) Llinares, J. M.; Powell, D.; Bowman-James, K. *Coord. Chem. Rev.* **2003**, *240*, 57−75. (f) Choi, K. H.; Hamilton, A. D. *Coord. Chem. Rev.* **2003**, *240*, 101−110. (g) Tomapatanaget, B.; Tuntulani, T.; Chailapakul, O. *Org. Lett.* **2003**, *5*, 1539−1542. (h) Sansone, F.; Baldini, L.; Casnati, A.; Lazzarotto, M.; Ugozzoli, F.; Ungaro, R. *Proc. Natl. Acad. Sci. U.S.A.* **2002**, *99*, 4842−4847.

(6) (a) Middel, O.; Verboom, W.; Reinhoudt, D. N. *Eur. J. Org. Chem.* **2002**, *16*, 2587−2597. (b) Droz, A. S.; Diederich, F. *J. Chem. Soc., Perkin Trans. 1* **2000**, 4224−4226. (c) Tamaru, S.; Shinkai, S.; Khasanov, A. B.; Bell, T. W. *Proc. Natl. Acad. Sci. U.S.A.* **2002**, *99*, 4972−4976. (d) Orner, B. P.; Salvatella, X.; Quesada, J. S.; De Mendoza, J.; Giralt, E.; Hamilton, A. D. *Angew. Chem., Int. Ed.* **2002**, *41*, 117−119. (e) Starnes, S. D.; Rudkevich, D. M.; Rebek, J. *J. Am. Chem. Soc.* **2001**, *123*, 4659−4669. (f) Almaraz, M.; Raposo, C.; Martin, M.; Caballero, M. C.; Moran, J. R. *J. Am. Chem. Soc.* **1998**, *120*, 3516−3517.

(7) (a) Mammen, M.; Choi, S.-K.; Whitesides, G. M. *Angew. Chem., Int. Ed.* **1998**, *37*, 2754−2794. (b) Lee, Y. C.; Lee, R. T. *Acc. Chem. Res.* **1995**, *28*, 321−327. (c) Lindhorst, T. K. *Top. Curr. Chem.* **2002**, *218*, 201−235.

(8) Amit, A. G.; Marinzza, R. A.; Phillips, S. E. V.; Poljak, R. J. *Science* **1986**, *233*, 747−753.

(9) Crego-Calama, M.; Timmerman, P.; Reinhoudt, D. N. *Angew. Chem., Int. Ed.* **2000**, *39*, 755−758.

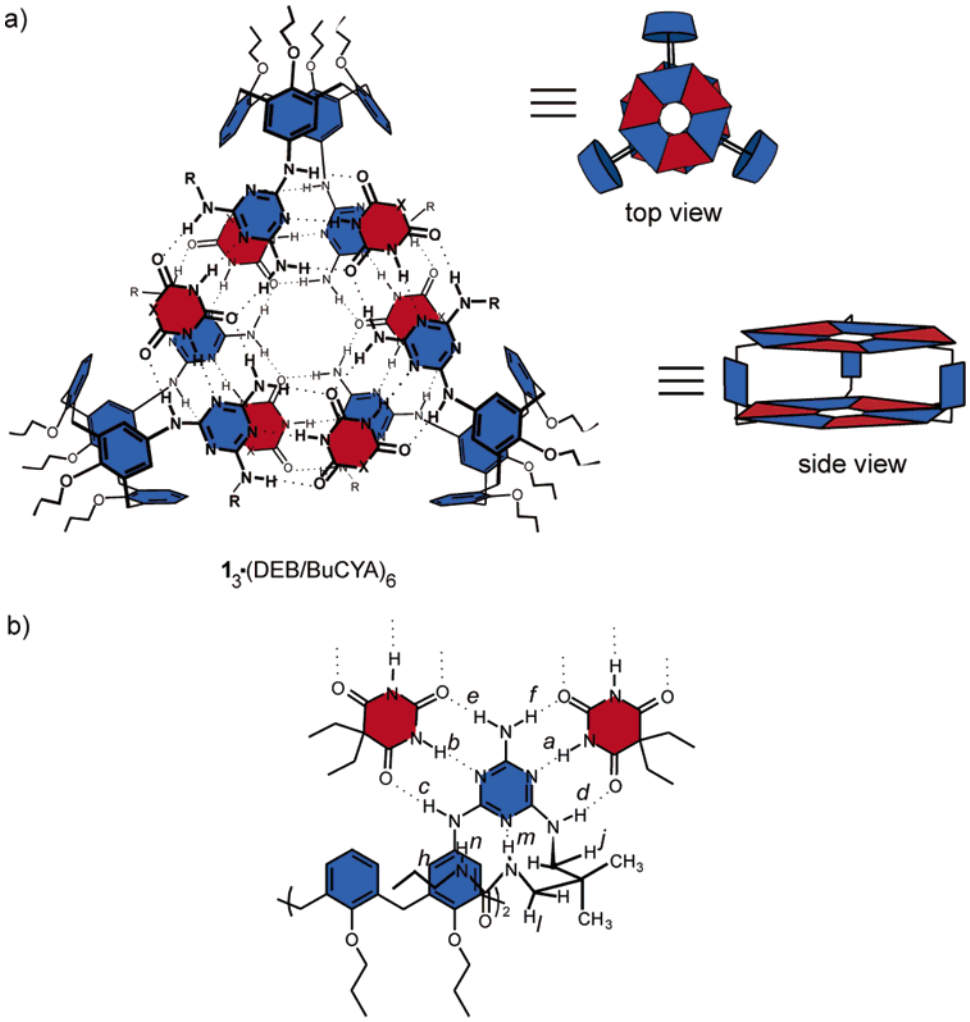

FIGURE 2. (a) Molecular structure of assemblies $\mathbf{1}_3$·(DEB/BuCYA)$_6$ (schematic top and side views are also included) and (b) part of the molecular structure of assembly $\mathbf{1}_3$·(DEB)$_6$ where the back folding of the side chain containing the ureido moiety is shown.

hydrogen-bonded receptors. Binding of *p*-nitrophenol (**4a**), diethylstilbestrol (DES, **4b**), and 2,2′-bis(4-hydroxyphenyl)propane (Bisphenol A, **4c**) to receptors $\mathbf{1}_3$·(DEB/BuCYA)$_6$, which bear six ureido moieties, was studied by ^{1}H NMR spectroscopy and isothermal titration microcalorimetry (ITC). Furthermore, the complexation of aromatic carboxylic acids (**5a**−**c**) by amino functionalized double rosette $\mathbf{2}_3$·(BuCYA)$_6$ and complexation of *n*-octyl-galactopyranoside (**6**) by Gly-L-Ser functionalized double rosette $\mathbf{3}_3$·(BuCYA)$_6$ were studied by similar techniques. The results show that the complementary recognition sites that are present on the assemblies are efficiently used to complex more than one guest.

Results and Discussion

Exo-receptors $\mathbf{1}$−$\mathbf{3}_3$·(DEB/BuCYA)$_6$ (Figure 1) are formed spontaneously by mixing the corresponding dimelamines **1**−**3** with 2 equiv of DEB or BuCYA in $CDCl_3$.[10]

Previous structural analysis of assemblies $\mathbf{1}_3$·(DEB/BuCYA)$_6$ by ^{1}H NMR spectroscopy using 2D DQF, TOCSY, and NOESY gave strong NOE connectivities between H_d and H_j and between H_l and H_m, respectively (Figure 2), indicating a rigid conformation of the 2,2′-dimethylpropyl side chain.[11] Furthermore, the signals for the two urea protons of $\mathbf{1}_3$·(DEB/BuCYA)$_6$ resonate at very different chemical shifts in the ^{1}H NMR spectrum (H_m = 5.2 and H_n = 2.4 ppm) suggesting that one of the urea protons is involved in hydrogen bonding with one of the nitrogen atoms of the triazine ring, causing the ureido moieties to fold back over the calix[4]arene aromatic ring. The result of this conformation is that the potential ureido recognition sites are (in principle) located at the top and the bottom of the double rosette assemblies $\mathbf{1}_3$·(DEB/BuCYA)$_6$.

For assembly $\mathbf{2}_3$·(BuCYA)$_6$ the 2,2′-dimethylpropyl chains should also give a certain preorganization of the complexing amino groups even though there is no evidence for extra hydrogen bonds. For assembly

(10) (a) Vreekamp, R. H.; Van Duynhoven, J. P. M.; Hubert, M.; Verboom, W.; Reinhoudt, D. N. *Angew. Chem., Int. Ed. Engl.* **1996**, *35*, 1215−1218. (b) Timmerman, P.; Vreekamp, R. H.; Hulst, R.; Verboom, W.; Reinhoudt, D. N.; Rissanen, K.; Udachin, K. A.; Ripmeester, J. *Chem. Eur. J.* **1997**, *3*, 1823−1832. (c) Kerckhoffs, J. M. C. A.; Ishi-I, T.; Paraschiv, V.; Timmerman, P.; Crego-Calama, M.; Shinkai, S.; Reinhoudt, D. N. *Org. Biomol. Chem.* **2003**, *1*, 2596−2603.

(11) Kerckhoffs, J. M. C. A.; Crego-Calama, M.; Luyten, I.; Timmerman, P.; Reinhoudt, D. N. *Org. Lett.* **2000**, *2*, 4121−4124.

$\mathbf{3}_3$·(BuCYA)$_6$, with Gly-L-Ser functionalities but lacking the preorganized chain, there is no evidence that the recognition sites are located at the top and the bottom of the double rosettes.

Complexation of Phenolic guests

Complexation of *p*-Nitrophenol. The complexation of *p*-nitrophenol (**4a**) by assembly $\mathbf{1}_3$·(BuCYA)$_6$ has been studied qualitatively by our group earlier using ^{1}H NMR spectroscopy ($CDCl_3$, 298 K) and MALDI-TOF mass spectrometry.[10c] Upon addition of 60 equiv of **4a** to double rosette $\mathbf{1}_3$·(BuCYA)$_6$ (1.0 mM) a ~0.45 and ~0.2 ppm downfield shift of urea protons H_m and H_n, respectively, is observed. The shifts for other rosette signals were much smaller (<0.08 ppm). These shifts are due to the formation of a hydrogen bond between the hydroxyl group of **4a** and the ureido carbonyl of $\mathbf{1}_3$·(BuCYA)$_6$. This was supported by the observation that no shifts of ureido protons H_m and H_n were observed when *p*-nitroanisole (having a methoxy group) was added to $\mathbf{1}_3$·(BuCYA)$_6$. Furthermore, the MALDI-TOF mass spectrum for the double rosette $\mathbf{1}_3$·(BuCYA)$_6$ (10 mM) and 10 equiv of **4a** shows that two main complexes, $\mathbf{1}_3$·(BuCYA)$_6$·$\mathbf{4a}_5$ and $\mathbf{1}_3$·(BuCYA)$_6$·$\mathbf{4a}_6$, are present in solution. These results indicated that a 1:6 complexation seems to be the most likely for complexation of **4a** by $\mathbf{1}_3$·(BuCYA)$_6$.

Here, the thermodynamic parameters associated with the binding of **4a** to $\mathbf{1}_3$·(BuCYA)$_6$ in 1,2-dichloroethane are determined via ITC measurements. The experiments were performed with 0.5 and 1.0 mM assembly $\mathbf{1}_3$·(BuCYA)$_6$ in the ITC cell while aliquots of **4a** (5 μL, 60 mM) were injected into the cell. Curve fitting of binding isotherms to a non-cooperative 1:6 binding model gave an intrinsic binding constant (K_i) of 422 ± 44 M^{-1} (Figure 3). Complexation of **4a** by $\mathbf{1}_3$·(BuCYA)$_6$ is enthalpy driven ($\Delta H° = -5.6 \pm 0.9$ kcal·mol^{-1} and $T\Delta S° = -2.0 \pm 1.0$ kcal·mol^{-1}), probably due to the formation of hydrogen bonds between the phenolic hydroxyl groups and the ureido moieties of the receptor.

Complexation of **4a** by $\mathbf{1}_3$·(BuCYA)$_6$ was also studied in increasingly more polar mixtures of $CD_3OD/CDCl_3$ by ^{1}H NMR spectroscopy (298 K). Complete rosette formation in $CD_3OD/CDCl_3$ mixtures was confirmed by ^{1}H NMR spectroscopy prior to the addition of **4a** to $\mathbf{1}_3$·(BuCYA)$_6$.[12] The ^{1}H NMR spectra of $\mathbf{1}_3$·(BuCYA)$_6$ (1.0 mM) with **4a** (20 equiv) were compared with the ^{1}H NMR spectra of $\mathbf{1}_3$·(BuCYA)$_6$ at each ratio $CD_3OD/CDCl_3$. The differences in chemical shift of the urea proton H_m (for H assignments see Figure 2) were plotted against the ratio $CD_3OD/CDCl_3$ (Figure 4). The observed chemical shift decreased rapidly when the ratio $CD_3OD/CDCl_3$ was increased. The interaction between the phenolic hydroxyl and the urea carbonyl is, therefore, weakened due to the competition for hydrogen bonding by methanol.

Complexation of Diethylstilbestrol (DES). Diethylstilbestrol (**4b**) is a synthetic estrogen synthesized to mimic the action of the estrogenic hormone estradiol in the body by binding to the estrogen receptor.[13] Diethylstilbestrol exists as an equilibrium mixture of 75% of the E-isomer and 25% of the Z-isomer.[14] It was reasoned that the two phenol moieties of **4b** should allow its recognition by the ureido moieties of $\mathbf{1}_3$·(BuCYA)$_6$.

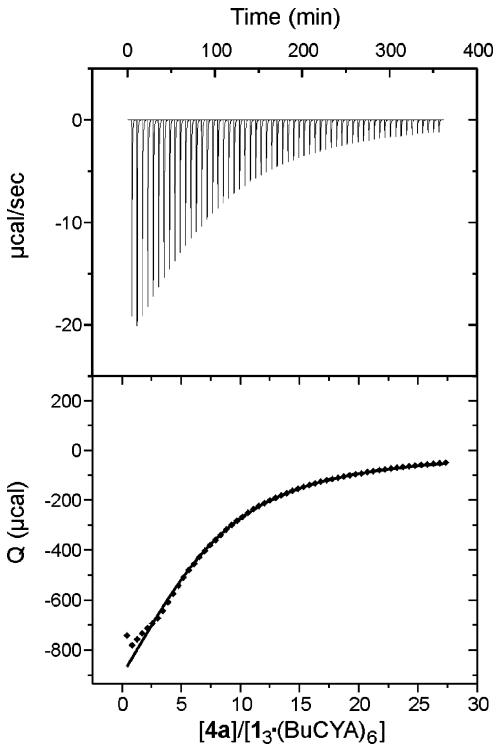

FIGURE 3. ITC measurement of 0.5 mM assembly $\mathbf{1}_3$·(BuCYA)$_6$ (host) with 60 mM **4a** (guest) at 25 °C. The plot shows the heat involved per injection of guest solution (5 μL) as function of the ratio [**4a**]/[$\mathbf{1}_3$·(BuCYA)$_6$]. The resulting binding isotherm is fitted to a noncooperative 1:6 binding algorithm.

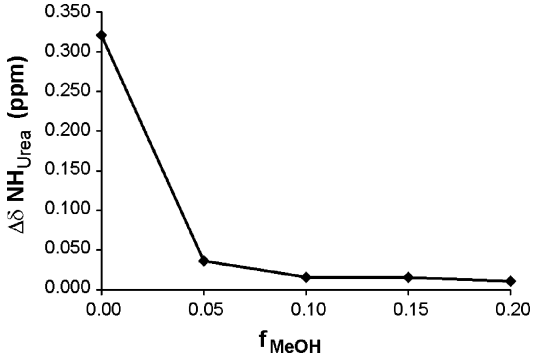

FIGURE 4. Differences in chemical shift for the ureido proton H_m (for H assignments see Figure 2b) of assembly $\mathbf{1}_3$·(BuCYA)$_6$ (1.0 mM) upon addition of **4a** (20 equiv) in a different solvent ratio $CD_3OD/CDCl_3$ (f_{MeOH}). The differences in the chemical shifts were calculated by comparison of the ^{1}H NMR spectra of the double rosette assembly $\mathbf{1}_3$·(BuCYA)$_6$ with and without **4a** at each solvent ratio.

The interaction between **4b** and double rosette $\mathbf{1}_3$·(BuCYA)$_6$ ($CDCl_3$, 298 K) was studied by ^{1}H NMR spectroscopy. Addition of 20 equiv of **4b** to $\mathbf{1}_3$·(BuCYA)$_6$ (1.0 mM) gave a 0.18 and a 0.07 ppm downfield shift

(12) Double rosette assemblies with urea functionalized dimelamine **2** are very stable in MeOH/$CHCl_3$ mixtures. ten Cate, M. G. J.; Crego-Calama, M.; Reinhoudt, D. N. *Org. Biomol. Chem.* **2005**, doi: 10.1039/b508449k.

(13) Meulenberg, E. P. *Eur. J. Lipid Sci. Technol.* **2002**, *104*, 131–136.

(14) Dai, Q. H.; Liu, X. *Chin. Sci. Bul.* **2000**, *45*, 2125–2129.

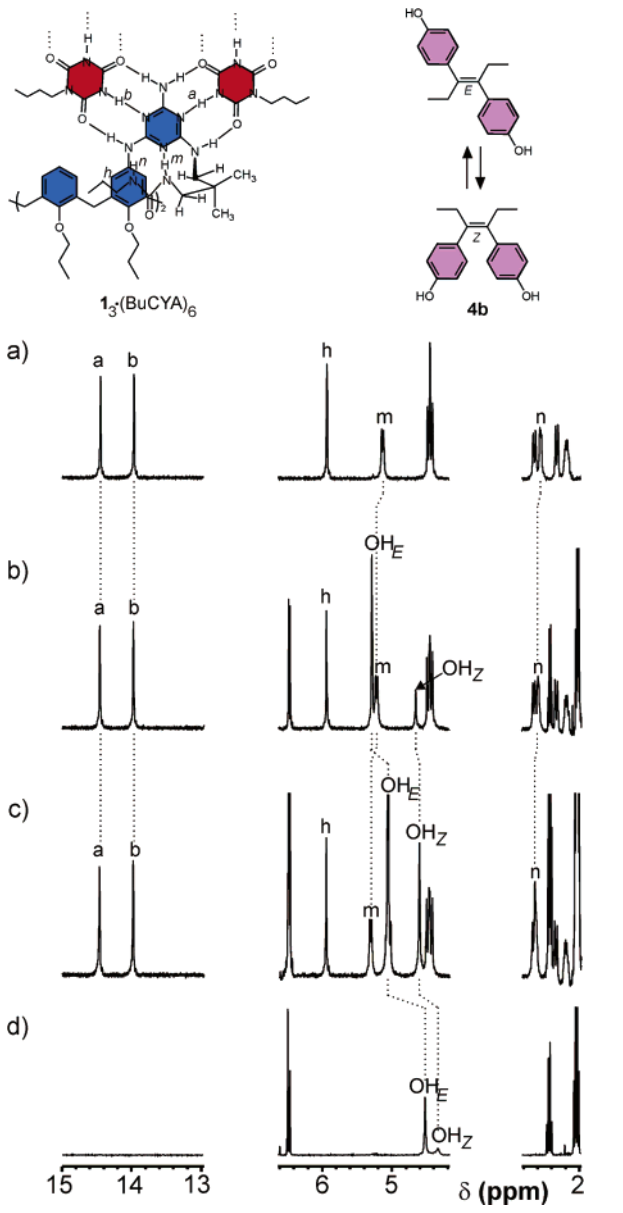

FIGURE 5. Parts of the ^{1}H NMR spectra of $\mathbf{1}_3$·(BuCYA)$_6$ (1 mM) in $CDCl_3$ at 298 K after addition of (a) 0, (b) 6, and (c) 20 equiv of **4b**, (d) part of ^{1}H NMR spectrum of **4b** (**4b** exists as a equilibrium mixture between 75% E-isomer and 25% Z-isomer).

of the ureido protons H_m and H_n, respectively (Figure 5a−c). No significant shifts were observed for the other hydrogen-bonded rosette signals (H_{c-f}).

In $CDCl_3$, the chemical shifts (δ) of the hydroxyl groups OH_E and OH_Z of **4b** (see Figure 1) are 4.49 and 4.30 ppm, respectively (Figure 5d). When 6 equiv of **4b** was added to $\mathbf{1}_3$·(BuCYA)$_6$ (1 mM) chemical shifts of 5.29 ($\Delta\delta = 0.80$ ppm) and 4.66 ppm ($\Delta\delta = 0.36$ ppm) were observed for the OH_E and OH_Z protons, respectively (Figure 5b). These differences in the chemical shifts are most likely due to the hydrogen bonding between the hydroxyl groups of **4b** and the ureido moieties of $\mathbf{1}_3$·(BuCYA)$_6$. Upon addition of 20 equiv of **4b** to $\mathbf{1}_3$·(BuCYA)$_6$ (1 mM) chemical shifts of 5.03 ($\Delta\delta = 0.54$ ppm) and 4.60 ppm ($\Delta\delta = 0.30$ ppm) were observed for OH_E and OH_Z, respectively (Figure 5c). These upfield shifts are the average of free and complexed **4b** in fast exchange in the NMR time scale.[15] Complexation of **4b** by the double rosette $\mathbf{1}_3$·(DEB)$_6$, formed with DEB, gave very similar results.

Dilution of a 1.0 mM solution of $\mathbf{1}_3$·(BuCYA)$_6$ and 20 equiv of **4b** in $CDCl_3$ to a 0.5 and a 0.1 mM assembly solution showed shifts of $H_{m,n}$ and $OH_{E,Z}$ in the ^{1}H NMR spectra. This excludes the possibility of proton transfer being responsible for the observed changes in the chemical shifts because proton transfer is independent of the initial concentration of host and guest.

Three different binding modes, i.e., 1:2, 1:3, and 1:6, can be envisioned for the complexation of **4b** by $\mathbf{1}_3$·(BuCYA)$_6$. In the 1:2 binding mode the guest molecules are situated on the top and the bottom of the double rosette platforms. In this binding mode only four ureido functionalities of $\mathbf{1}_3$·(BuCYA)$_6$ are used to bind the **4b** molecules (Figure 6), but additional $\pi-\pi$ interactions of **4b** with the aromatic rosette platforms are possible. Gas-phase molecular modeling calculations (Quanta 97, CHARm 24.0) indicated that the distance between the two hydroxyl groups of **4b** is large enough to allow ditopic binding of one molecule **4b** to two different ureido moieties in each rosette plane (1:2 binding). Nevertheless, a detailed study of the ^{1}H NMR spectra and the symmetry of the complex exclude this mode of binding. The complexation of two molecules of **4b** to the double rosette $\mathbf{1}_3$·(BuCYA)$_6$ would break the D_3-symmetry of the rosette assembly (see Figure 6). The D_3-isomer has two signals for the hydrogen-bonded NH_{DEB} protons H_a and H_b because the three dimelamines in the assembly are identical (Figure 5a). If **4b** would bind ditopically to $\mathbf{1}_3$·(BuCYA)$_6$, the assembly will lose its C_3-axis (Figure 6) and a complex with C_2-symmetry will be obtained. This results in different chemical shifts for each of the H_a and the H_b protons in the same rosette[16] floor and six signals should appear in the ^{1}H NMR spectrum in the region of 13−15 ppm. On the other hand, if the guest molecules are complexed by $\mathbf{1}_3$·(BuCYA)$_6$ in fast exchange, the average symmetry of the 1:2 complex would not break the D_3-symmetry of the rosette assembly and two signals should be observed; nevertheless, it is expected that these signals are shifted compared to the NH_{DEB} protons H_a and H_b of the free assembly $\mathbf{1}_3$·(BuCYA)$_6$ due to interactions with the aromatic rings present in **4b** (see also complexation of aromatic carboxylic acids). Only two nonshifted signals in the region 13−15 ppm are observed for the hydrogen-bonded rosette protons H_a and H_b in the ^{1}H NMR spectrum when **4b** is added to $\mathbf{1}_3$·(BuCYA)$_6$; thus, it is not likely that **4b** binds to $\mathbf{1}_3$·(BuCYA)$_6$ in a 1:2 ratio.

In the 1:6 binding mode (Figure 6) one molecule **4b** is bound to each ureido moiety via one hydrogen bond. In the 1:3 binding mode each molecule of **4b** forms two hydrogen bonds, one with the ureido moiety at the top floor and one with the ureido at the bottom floor of double rosette assembly $\mathbf{1}_3$·(BuCYA)$_6$ (Figure 6).[17] For both, the 1:3 and 1:6 binding modes, all the six ureido functionalities of $\mathbf{1}_3$·(BuCYA)$_6$ are used to bind **4b**. In these two

(15) Ratio free/bound guest is higher when 20 equiv is added.

(16) H_a and H_b in one rosette are homotopic compared to the corresponding H_a and H_b in the other rosette floor when two molecules of **4b** would bind to the assembly $\mathbf{1}_3$·(BuCYA)$_6$.

(17) In this case the binding sites have to turn away from the rosette platform.

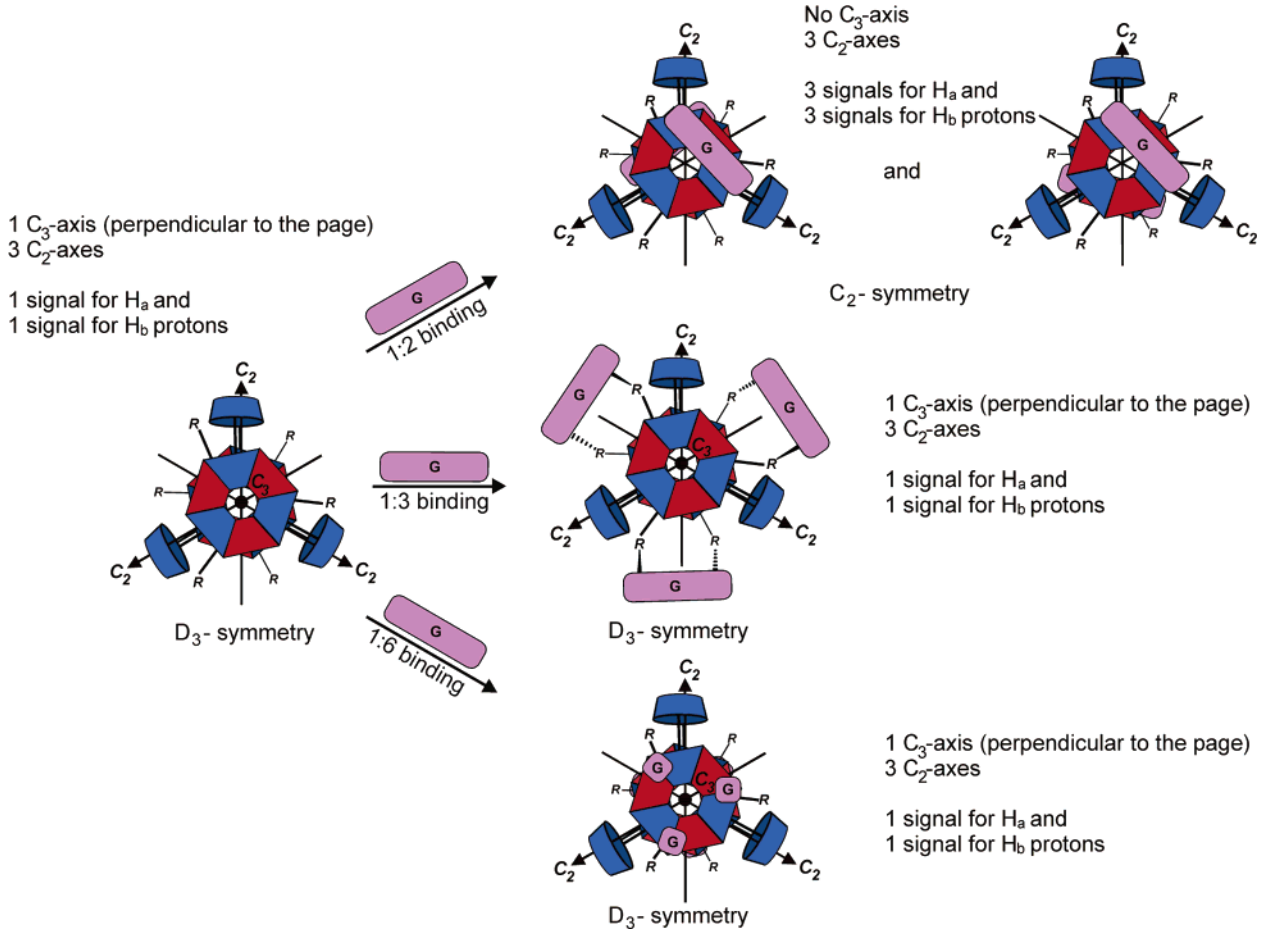

FIGURE 6. Schematic illustration of 1:2, 1:3, and 1:6 binding modes for the complexation of **4b** (G) by the assembly $\mathbf{1}_3$·(BuCYA)$_6$ (top view). For 1:6 binding another three guest molecules are bound to the second rosette floor, which are not clearly visible in the graphical representation.

binding modes, complexation of **4b** will not break the D_3-symmetry of the double rosette assembly $\mathbf{1}_3$·(BuCYA)$_6$; therefore, only two signals for H_a and H_b in the ^{1}H NMR spectrum are expected. Thus, based on the ^{1}H NMR results (Figure 5; only two signals), both binding modes are possible. The 1:3 binding mode is probably preferred if the driving force for complexation of DES is only hydrogen bonding (most efficient use of binding sites). This mode of binding was previously observed for complexation of chiral dicarboxylic acids by pyridyl functionalized double rosette assemblies.[18]

The binding affinity of **4b** to $\mathbf{1}_3$·(BuCYA)$_6$ was determined by ^{1}H NMR titration experiments in $CDCl_3$ (1 mM, 298 K). The chemical shift of H_m was monitored during the titration experiments. Curve fitting of the induced shifts as a function of the **4b**:$\mathbf{1}_3$·(BuCYA)$_6$ ratio to a 1:3 and 1:6 binding model gave K_i values of 84 and 119 M^{-1}, respectively.

The complexation of **4b** by $\mathbf{1}_3$·(BuCYA)$_6$ was also studied using ITC. Measurements in 1,2-DCE (298 K) with **4b** (6 mM) inside the ITC cell and $\mathbf{1}_3$·(BuCYA)$_6$ (20 mM) as titrant gave K_i values of 161 and 56 M^{-1} after fitting of the ITC data to a 1:3 and 1:6 binding algorithm, respectively (Table 1). Furthermore, in neat 1,2-DCE, complexation of **4b** by $\mathbf{1}_3$·(BuCYA)$_6$ is enthalpy driven (Table 1). The $\Delta H°$ values are −10.5 and −12.0 kcal·mol^{-1} for 1:3 and 1:6 binding, respectively.

TABLE 1. Thermodynamic Parameters Determined by ITC (298 K) for the Complexation of 4a−c by Assembly $\mathbf{1}_3$·(BuCYA)$_6$ in 1,2-DCE

guest	binding mode	K_i (M^{-1})	$\Delta H°$ (kcal·mol^{-1})	$\Delta G°$ (kcal·mol^{-1})	$T\Delta S°$ (kcal·mol^{-1})
4a	1:6	422 ± 44	−5.6 ± 0.9	−3.6 ± 0.1	−2.0 ± 1.0
4b[a]	1:3	161	−10.5	−3.0	−7.5
	1:6	56	−12.0	−2.4	−9.6
4c	1:3	113 ± 4	−10.1 ± 0.4	−2.9 ± 0.1	−7.2 ± 0.4
	1:6	(no fit)			

[a] ITC measurement was performed at one concentration only.

Comparison of the $\Delta H°$ for the binding of **4a** and **4b** to $\mathbf{1}_3$·(BuCYA)$_6$ (Table 1) indicates the formation of two hydrogen bonds and, thus, a 1:3 binding of **4b** to $\mathbf{1}_3$·(BuCYA)$_6$. For the 1:3 binding mode one molecule **4b** forms two hydrogen bonds with $\mathbf{1}_3$·(BuCYA)$_6$. The average enthalpy value for the formation of a single hydrogen bond is then −5.3 kcal·mol^{-1}. This value is comparable with $\Delta H°$ for the binding of **4a**, that can form only one hydrogen bond, to $\mathbf{1}_3$·(BuCYA)$_6$ (−5.6 kcal·mol^{-1}). The larger gain in $\Delta H°$ due to the formation of two hydrogen bonds is, however, accompanied by a larger unfavorable entropic contribution. As a consequence, ditopic binding

(18) ITC measurements were performed with four different concentrations of assembly $\mathbf{2}_3$·(BuCYA)$_6$ (0.25, 0.50, 0.375, 1.0 mM) in the cell and **5c** as titrant (20, 25, 40, and 60 mM, respectively).

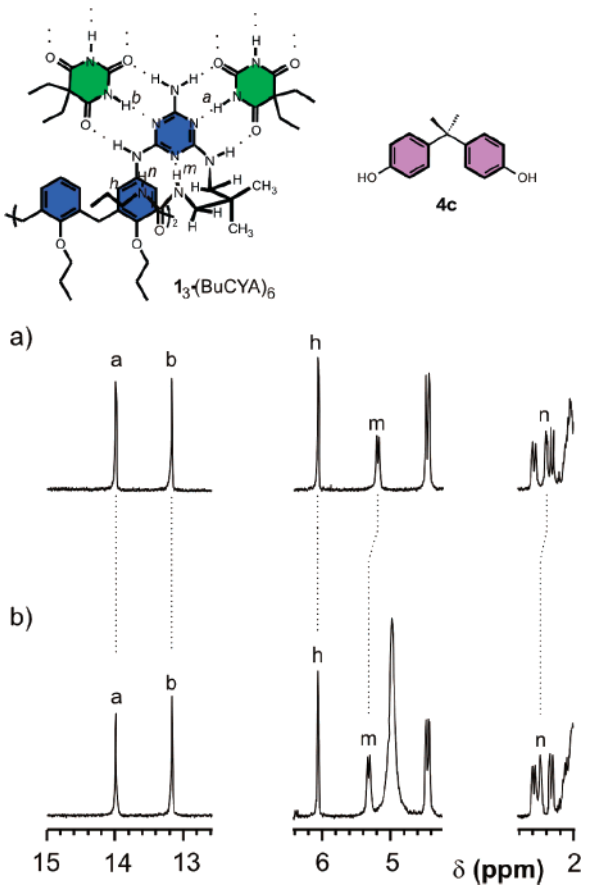

FIGURE 7. Parts of the ^{1}H NMR spectra of $\mathbf{1}_3$·(DEB)$_6$ (1 mM) in $CDCl_3$ at 298 K after addition of (a) 0 and (b) 20 equiv of **4c**.

of **4b** to $\mathbf{1}_3$·(BuCYA)$_6$ does not increase the affinity as compared to **4a**.

Complexation of Bisphenol A. 2,2-Bis(4-hydroxyphenyl)propane (Bisphenol A, **4c**) is another synthetic ligand for the natural estrogen receptor[19] which also has two phenol moieties like **4b** but these are not conjugated. Binding of **4c** to $\mathbf{1}_3$·(DEB)$_6$ and $\mathbf{1}_3$·(BuCYA)$_6$ was first studied using ^{1}H NMR spectroscopy. The addition of 20 equiv of **4c** to $\mathbf{1}_3$·(DEB)$_6$ (1.0 mM) gave a 0.14 ppm downfield shift of ureido proton H_m and a 0.09 ppm downfield shift of ureido proton H_n (Figure 7). No significant shifts were observed for the hydrogen-bonded rosette signals and only one set of signals was observed for H_a and H_b in the ^{1}H NMR spectrum. These results indicate that the 1:2 binding mode, as concluded for **4b**, can be excluded. The intrinsic binding constants (K_i) are 155 and 395 M^{-1} for the 1:3 and 1:6 binding modes, respectively.

ITC measurements (1.0 mM assembly in the ITC cell and 60 mM **4c** in the buret, 1,2-DCE, 298 K) gave a K_i value of 113 M^{-1} after fitting to 1:3 binding model, while an accurate fit to a 1:6 binding model was not possible (see Table 1). Furthermore, $\Delta H°$ and $T\Delta S$ values of −10.1 and −7.2 kcal·mol^{-1}, respectively, were obtained for the 1:3 binding of **4c** to $\mathbf{1}_3$·(BuCYA)$_6$.

(19) Steinmetz, R.; Brown, N. G.; Allen, D. L.; Bigsby, R. M.; BenJonathan, N. *Endocrinology* **1997**, *138*, 1780−1786.

Complexation of Aromatic Carboxylic Acids. Binding of 3-(2-furyl)propanoic acid (**5a**, Figure 8a), *trans*-cinnamic acid (**5b**, Figure 8b), and *trans*-benzoylbutenoic acid (**5c**, Figure 8c) (10 equiv) to receptor $\mathbf{2}_3$·(BuCYA)$_6$ (1.0 mM), which has amino moieties, was studied using ^{1}H NMR spectroscopy ($CDCl_3$, 298 K) and ITC (1,2-DCE 298 K). The amino groups of receptor $\mathbf{2}_3$·(BuCYA)$_6$ are expected to bind with the carboxylic acid groups of guests **5a**−**c**.

The interaction between $\mathbf{2}_3$·(BuCYA)$_6$ with guests **5a**−**c** becomes apparent from the shifts of several hydrogen-bonded protons in the ^{1}H NMR spectra (Figure 8). These shifts are very clear for the hydrogen-bonded rosette protons H_{a-d}. For example, H_a shifted 0.23, 0.26, and 0.35 ppm upfield when 10 equiv of **5a**, **5b**, and **5c**, respectively, was added to a 1.0 mM solution of $\mathbf{2}_3$·(BuCYA)$_6$ in $CDCl_3$. Also the double doublets of the calix[4]arene bridge protons H_i (4.3−4.6 ppm) shifted when 10 equiv of **5a**, **5b**, or **5c** was added (Figure 8). Furthermore, the amino protons of assembly $\mathbf{2}_3$·(BuCYA)$_6$ shift from about 2 ppm to 5−6.5 ppm. This observed broad signal around 5−6.5 ppm is probably due to hydrogen bonding between the amino groups of $\mathbf{2}_3$·(BuCYA)$_6$ and the carboxylic acid groups of the guests **5a**−**c** (NH_2···HOOC).

Dilution of a 5.0 mM solution of $\mathbf{2}_3$·(BuCYA)$_6$ and 6 equiv of **5a** in $CDCl_3$ to 2.5, 1.0, 0.5. and 0.25 mM gave clear shifts for the NH_2···HOOC signal. This excludes proton transfer being responsible for the observed chemical shifts.

Furthermore, upon complexation of guest **5a**−**c** with $\mathbf{2}_3$·(BuCYA)$_6$ large shifts are observed for the guest protons H_{1-5} (Table 2). The large shifts observed for H_{1-3} are probably due to $\pi-\pi$ interactions of the aromatic rings of **5a**−**c** with the rosette platforms, while the higher shifts observed for $H_{4,5}$ of **5a**−**c** indicate also an interaction between the carboxylic acid moiety of the guest and the amino groups of $\mathbf{2}_3$·(BuCYA)$_6$.

Summarizing, the ^{1}H NMR data indicate that binding of **5a**−**c** to $\mathbf{2}_3$·(BuCYA)$_6$ occurs through hydrogen bonding between the amino functionality of the host and the carboxylic acid moiety of the guests. Furthermore, the shifts of the hydrogen-bonded protons H_{a-d} observed upon complexation of **5a**−**c** are probably due to interactions between the aromatic moieties of the guests (located on top and bottom) with the rosette platforms. This hypothesis is supported by the shifts of protons H_{1-5} of the guest molecules **5a**−**c** upon complexation with $\mathbf{2}_3$·(BuCYA)$_6$.

ITC measurements using 0.25, 0.5, and 1.0 mM solutions of $\mathbf{2}_3$·(BuCYA)$_6$ in the ITC cell and 25, 30, and 60 mM **5a** in 1,2-DCE as titrant, respectively, gave an intrinsic binding constant of 3500 M^{-1} for the complexation of **5a** by $\mathbf{2}_3$·(BuCYA)$_6$ after fitting to an independent 1:6 binding model (Figure 9a; Table 3). Fitting of ITC data to 1:2 and 1:4 models was not possible. Complexation of **5a** by $\mathbf{2}_3$·(BuCYA)$_6$ is enthalpy driven ($\Delta H° = -6.3 \pm 0.4$ kJ·mol^{-1}, $T\Delta S = -1.5 \pm 0.2$ kJ·mol^{-1}). Similar measurements with **5b** using 0.25, 0.375, 0.5, and 1.0 mM solutions of $\mathbf{2}_3$·(BuCYA)$_6$ in the ITC cell and 20, 25, 30, and 50 mM **5b** in 1,2-DCE as titrant, respectively, gave a K_i value of 1799 M^{-1} (Figure 9b; Table 3). Complexation of **5b** by $\mathbf{2}_3$·(BuCYA)$_6$ is also enthalpy driven ($\Delta H° = -5.6 \pm 2.0$ kJ·mol^{-1}, $T\Delta S = -1.2 \pm 0.4$ kJ·mol^{-1}).

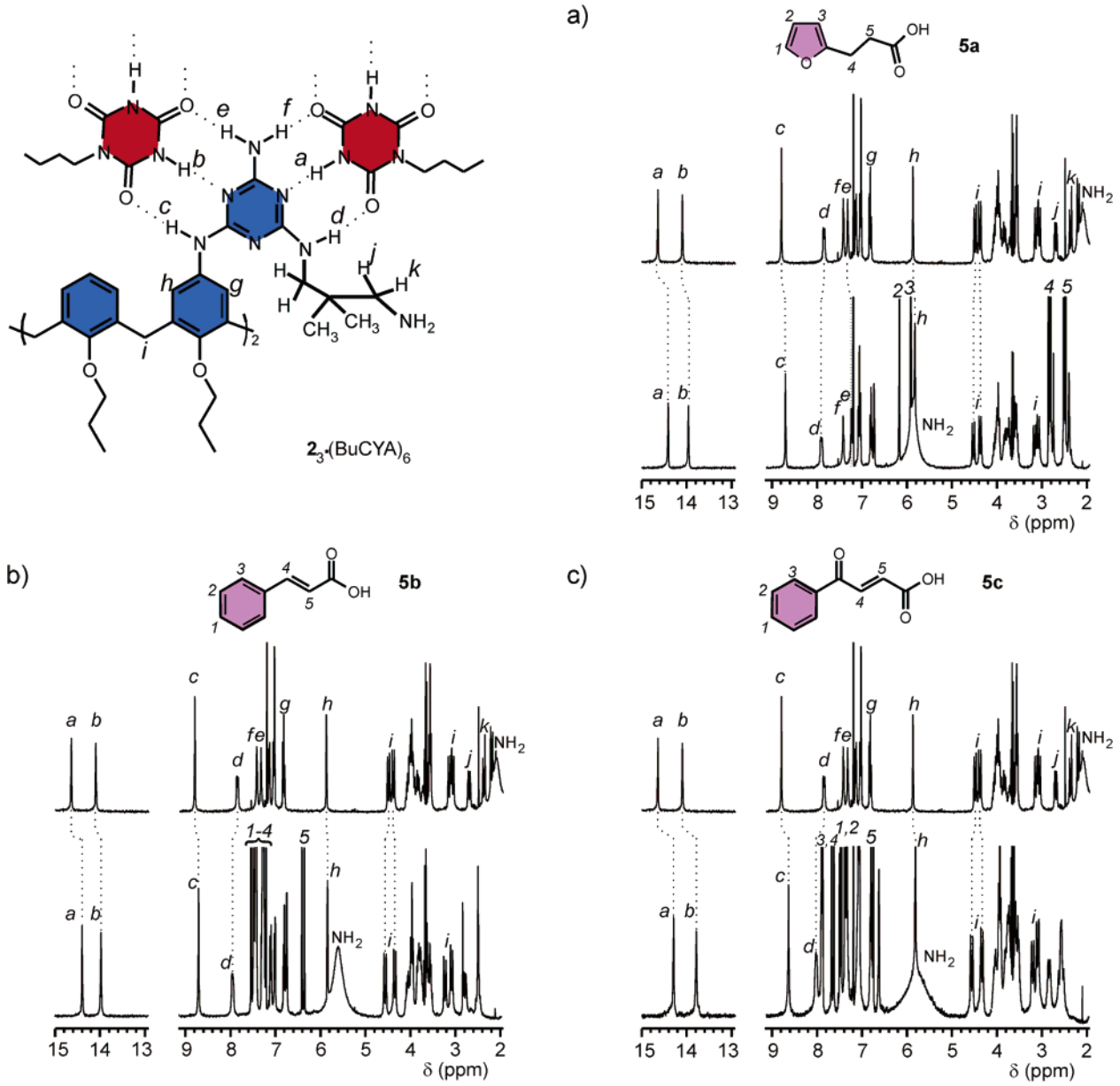

FIGURE 8. Parts of the ^{1}H NMR spectra of (a) 1.0 mM $\mathbf{2}_3$·(BuCYA)$_6$ (top) and after addition of 10 equiv of **5a** (bottom), (b) 1.0 mM $\mathbf{2}_3$·(BuCYA)$_6$ (top) and after addition of 10 equiv of **5b** (bottom), (c) 1.0 mM $\mathbf{2}_3$·(BuCYA)$_6$ (top) and after addition of 10 equiv of **5c** (bottom). Spectra were recorded in $CDCl_3$ at 298 K.

Fitting of the measured ITC data for the complexation of **5c** by $\mathbf{2}_3$·(BuCYA)$_6$ to an appropriate model was not possible. Therefore, ^{1}H NMR titrations were performed to study the value of K_i for the complexation of this guest by assembly $\mathbf{2}_3$·(BuCYA)$_6$.

^{1}H NMR titration of $\mathbf{2}_3$·(BuCYA)$_6$ with **5c** gave a K_i value of 563 M^{-1} when the induced shifts of the NH_2 protons were fitted to a 1:6 binding model (Figure 10a). However, induced shifts of the hydrogen-bonded H_c protons (see Figure 8 for proton assignment) could only be fitted in a dependent 1:6 binding model (Figure 10b), with binding constants of 38, 29, 271, 299, 1057, and 3808 M^{-1} for K_{1-6}, respectively. The increase in binding affinity indicates a positive cooperative effect upon binding of **5c**, possibly due to conformational changes of the double rosette $\mathbf{2}_3$·(BuCYA)$_6$.

Binding of *n*-Octylgalactopyranoside. Carbohydrates act as substrates for specific receptors in a wide range of biological processes.[7a,20] Thus, artificial receptors that can recognize and bind specific saccharides are receiving increased attention.[21] Since the affinity of a single carbohydrate unit for its receptor is often low, strong binding is achieved by the simultaneous interaction of several identical glycoside residues with the receptor (often proteins) that has several equivalent binding sites.[22]

Binding of *n*-octylgalactopyranoside (**6**; Figure 11) to $\mathbf{3}_3$·(BuCYA)$_6$, with Gly-L-Ser functionalities, was studied

(20) Varki, A. *Glycobiology* **1993**, *3*, 97−130.
(21) Fredericks, J. R.; Hamilton, A. D. In *Comprehensive Supramolecular Chemistry*; Atwood, J. L., Davies, J. E. D., MacNicol, D. D., Vögte, F., Eds.; Elsevier: Oxford, England, 1996; Vol. 9, pp 565−594.

TABLE 2. Upfield Shift of Protons H_{1-5} of 5a−c after Addition of 10 Equiv of Guest to Assembly 2_3·(BuCYA)$_6$ (1.0 mM).[a]

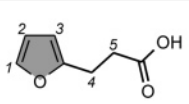
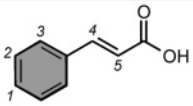
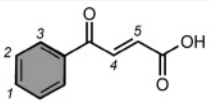

H	Δδ (ppm) **5a**	Δδ (ppm) **5b**	Δδ (ppm) **5c**
1	-	0.062	0.164
2	0.042	0.098	0.170
3	0.060	0.070	0.123
4	0.080	0.205	0.338
5	0.148	0.240	0.122

[a] ^{1}H NMR Spectra Were Recorded in $CDCl_3$ at 298 K

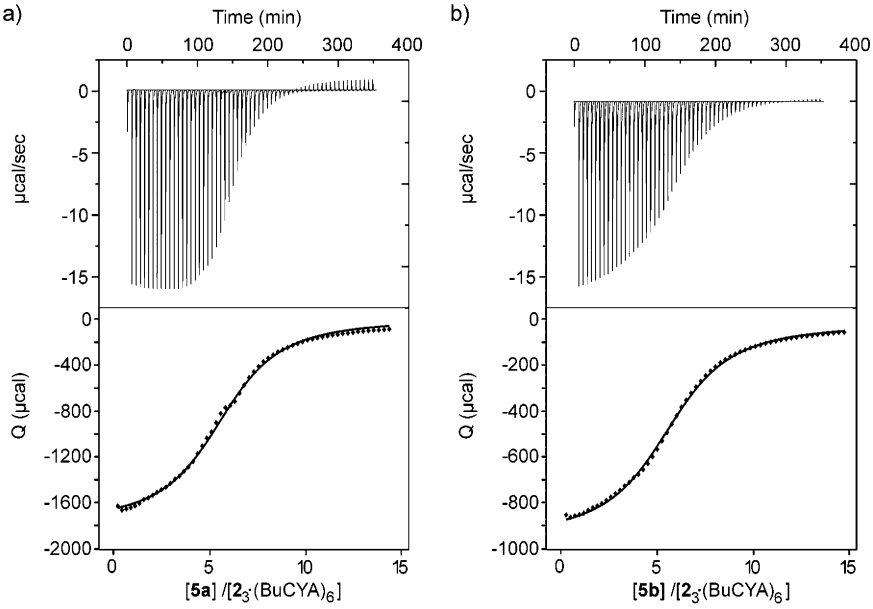

FIGURE 9. ITC measurement of (a) assembly $\mathbf{2}_3$·(BuCYA)$_6$ (1.0 mM) with **5a** (60 mM) and (b) assembly $\mathbf{2}_3$·(BuCYA)$_6$ (0.375 mM) with **5b** (25 mM) at 25 °C. The plots show the heat involved per injection of titrant (5 μL) as function of [guest]/[assembly]. The resulting binding isotherms are curve fitted to a noncooperative 1:6 binding algorithm.

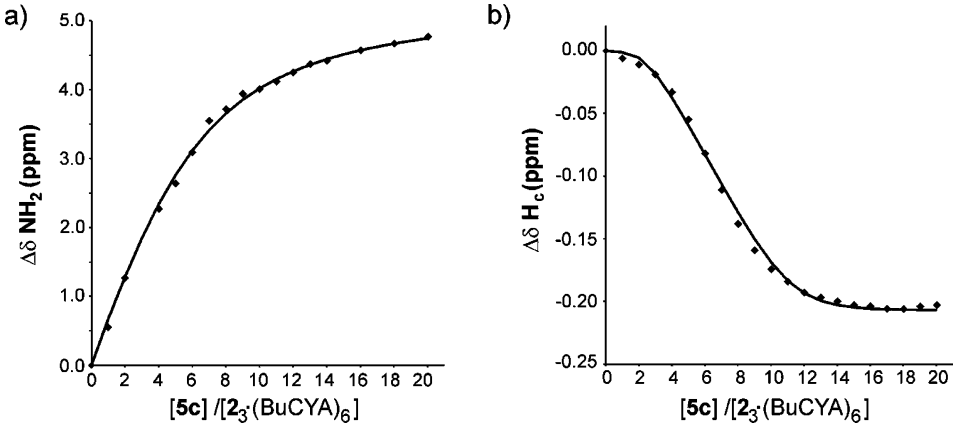

FIGURE 10. Plots of the ^{1}H NMR induced shifts of the (a) NH_2 protons and (b) H_c protons during the titration of $\mathbf{2}_3$·(BuCYA)$_6$ with **5c** versus [**5c**]/[$\mathbf{2}_3$·(BuCYA)$_6$]. The induced shifts are fitted in an (a) independent and (b) dependent 1:6 binding model.

using ^{1}H NMR spectroscopy ($CDCl_3$, 298 K). The interaction between **6** and $\mathbf{3}_3$·(BuCYA)$_6$ becomes apparent from the shifts of the OH protons of the serine and the OH protons of **6** (Figure 11). Upon addition of 10 equiv of **6** to $\mathbf{3}_3$·(BuCYA)$_6$ (1.0 mM) the signal of the serine hydroxyl group (H_i) shifts 0.57 ppm downfield, probably as a result

TABLE 3. Thermodynamic Parameters for the Complexation of 5a−c by Assembly 2_3·(BuCYA)$_6$ in 1,2-DCE

guest	binding mode	K_i (M^{-1})	$\Delta H°$ (kcal·mol^{-1})	$\Delta G°$ (kcal·mol^{-1})	$T\Delta S°$ (kcal·mol^{-1})
5a	1:6	3500 ± 929	−6.3 ± 0.4	−4.8 ± 0.2	−1.5 ± 0.2
5b	1:6	1799 ± 211	−5.6 ± 2.0	−4.4 ± 0.1	−1.2 ± 0.4
5c[a]	1:6	563			

[a] Data obtained from induced shifts of the NH_2 protons in the ^{1}H NMR titration measurement in $CDCl_3$.

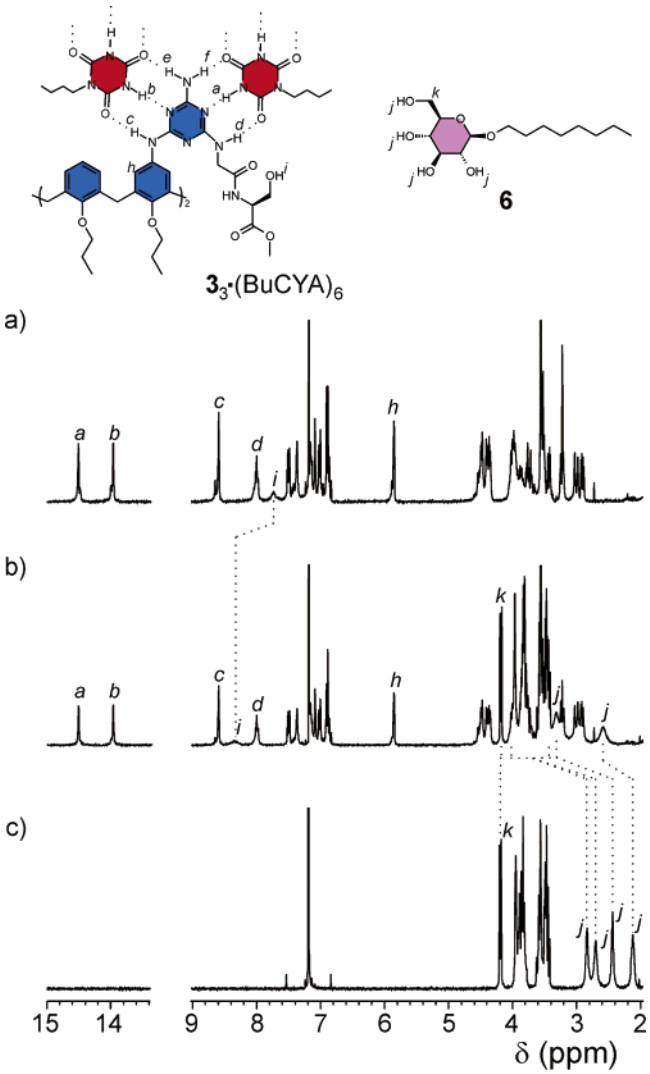

FIGURE 11. Parts of the ^{1}H NMR spectra of (a) $\mathbf{3}_3$·(BuCYA)$_6$ (1.0 mM), (b) $\mathbf{3}_3$·(BuCYA)$_6$ (1.0 mM) and 10 equiv **6**, and (c) **6** (10 mM) and molecular structures of $\mathbf{3}_3$·(BuCYA)$_6$ and **6**. Spectra were recorded in $CDCl_3$ at 298 K.

of hydrogen bonding. After guest addition all the hydroxyl groups of **6** (H_j) are shifted downfield but only two signals at 3.32 and 2.60 ppm ($\Delta\delta$ = 0.47 and 0.88 ppm, respectively) remain visible because the other two H_j protons are under the rosette signals (between δ = 3.3 and 3.9 ppm).

It is unclear how **6** binds to $\mathbf{3}_3$·(BuCYA)$_6$, but the ^{1}H NMR results indicate that probably all four hydroxyl

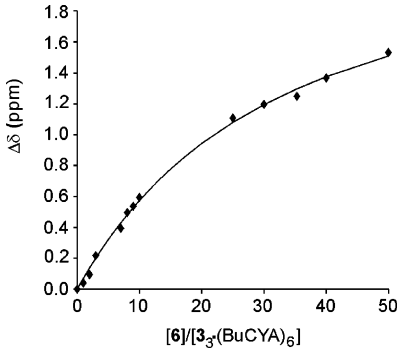

FIGURE 12. Plot of the ^{1}H NMR induced shifts ($\Delta\delta$ OH_{Ser}) during titration of $\mathbf{3}_3$·(BuCYA)$_6$ with **6** versus [**6**]/[$\mathbf{3}_3$·(BuCYA)$_6$]. The induced shifts are fitted in a 1:6 binding model to calculate the intrinsic binding constant K_i.

groups are involved in hydrogen bonding. Therefore, binding constants were calculated for 1:2, 1:3, 1:4, and 1:6 binding modes.[23]

^{1}H NMR titration experiments gave intrinsic K_i values of 31, 32, 34, and 37 M^{-1} for 1:2, 1:3, 1:4, and 1:6 binding, respectively (Figure 12). Unfortunately, ITC measurements could not be performed due to gelation at high concentrations of **6** in 1,2-DCE. These results indicate that assembly $\mathbf{3}_3$·(BuCYA)$_6$ binds **6** probably via formation of hydrogen bonds between the serine hydroxyl groups of the receptor and the hydroxyl groups of guest **6** with low affinity.

Conclusions

Exo-complexation of multiple guests by double rosette assemblies is observed. The results show that recognition sites located at the periphery of double rosette assemblies are used efficiently, i.e., minimum number of guests with maximum use of recognition sites.

For exo-receptor $\mathbf{1}_3$·(BuCYA)$_6$ and *p*-nitrophenol (**4a**) a 1:6 binding mode was observed by single hydrogen bonding with each guest molecule, while a 1:3 binding mode was observed for diethylstilbestrol (**4b**) and 2,2-bis(4-hydroxyphenyl)propane (**4c**) where each guest molecule is forming two hydrogen bonds with two urea moieties at the first and the second floor of the double rosette assembly $\mathbf{1}_3$·(BuCYA)$_6$. Binding affinities of 422, 161, and 113 M^{-1} were determined for binding of **4a**, **4b**, and **4c**, respectively. Even though it can be concluded from the thermodynamic data that ditopic binding of **4b** and **4c** to $\mathbf{1}_3$·(BuCYA)$_6$ does not increase the binding affinity compared to **4a**, it should be emphasized that **4a** is a much stronger acid and a better hydrogen bond donor than carbon-substituted phenols, such as those in **4b** and **4c**. Therefore, these results could indicate that, indeed, the ditopic binding would improve the relative affinity when compared to carbon-substituted phenols.

Aromatic carboxylic acids **5a−c** bind with exo-receptor $\mathbf{2}_3$·(BuCYA)$_6$ in a 1:6 binding mode. Binding of these guests involved hydrogen bonding between amino groups of the receptor and carboxylic acid groups of the guests and organization of the guest molecules at the top and

(22) Casnati, A.; Sansone, F.; Ungaro, R. *Acc. Chem. Res.* **2003**, *36*, 246−254.

(23) 1:1 and 1:5 binding modes are unlikely because they suggest differences in binding affinity between the recognition groups at the top and bottom of assembly $\mathbf{3}_3$·(BuCYA)$_6$.

the bottom of the receptor. Binding affinities of 3500 M^{-1} and 1799 M^{-1} were determined for binding of **5a** and **5b**, respectively. The binding affinities obtained for **5c** indicate a positive cooperative effect, possibly due to conformational changes of the double rosette $\mathbf{2}_3$·$(BuCYA)_6$.

Exo-receptor $\mathbf{3}_3$·$(BuCYA)_6$ binds *n*-octylgalactopyranoside ($K_i = 31-37\ M^{-1}$), possibly by formation of hydrogen bonds between the serine hydroxyl of the receptor and hydroxyl groups of the carbohydrate guest.

These examples show that structural diversity within the exo-receptors, generated by the different functionalities, allows the complexation of different biologically important molecules via different binding motifs, resembling the approach exhibited by natural receptors such as antibodies.

Experimental Section

All chemicals were reagent grade and used without further purification. The synthesis of **1**, **2**, and **3** are described elsewhere.[10,11] ^1H NMR spectra were recorded on a ^1H NMR 300 MHz spectrometer in CD_3OD or $CDCl_3$. Residual solvent protons were used as internal standard, and chemical shifts are given relative to trimethylsilane (TMS). Calorimetric measurements were carried out using a VP−ITC microcalorimeter with a cell volume of 1.4115 mL. For each experiment the heat effect of 60 injections of 5 μL of titrant was measured. Instrument settings were injection duration of 30 s, spacing of 570 s, and low feedback at 16.3 μcal/s reference power and a temperature of 25 °C.

Acknowledgment. Dr. M. G. J. ten Cate and Dr. M. Crego-Calama acknowledge the Technology Foundation of The Netherlands (CW-STW) and Royal Netherlands Academy of Arts and Science (KNAW) for financial support.

JO051218C